Journal of Applied Polymer Science

An effective intumescent flame retardancy of LDPE induced by the combination of APP and CNCO-HA

Caimin Feng, Minyi Liang, Jiali Jiang, Yikun Zhang, Jianguang Huang, Hongbo Liu
Department of applied chemical engineering, College of Applied Chemical Engineering, Shunde Polytechnic, Foshan 528333, China
Minyi Liang contributed equally to this work and should be considered co-first author.
Correspondence to: J. Huang (E-mail: hjguang@139.com) and H. Liu (E-mail: 76094406@qq.com)

ABSTRACT: A char-forming agent poly(4,6-dichloro-N-hydroxyethyl−1,3,5-triazin-2-amine-1,6-diaminohexane) (CNCO-HA) containing triazine rings was chosen for improving the flame retardant of low density polyethylene (LDPE). The synergistic effect of CNCO-HA and Ammonium polyphosphate (APP) on the flame retardancy and char-forming behavior of LDPE were investigated. The limited oxygen index (LOI) and vertical burning test (UL-94) results indicated the optimal weight ratio of APP to CNCO-HA was 3:1, and the LOI value of composite reached 31.0% with 30% intumescent flame retardant (IFR) loading. The cone calorimeter test analysis revealed that IFR presented excellent char forming and smoke suppression ability, and resulted in the efficient decrease of combustibility parameters. The thermogravimetric analysis results demonstrated that IFR reduced the thermal degradation rate at main stage of degradation. Scanning electron microscopy observed that IFR promoted to form a compact and continuous intumescent char layer. The Laser Raman spectroscopy spectra showed that larger graphitization degree was formed to enhance the strength of char, and Fourier transform infrared results presented that P-O-C and P-O-P structures in the residue char were formed to improve shield performance of the char layer to obtain better flame retardant properties of the composite. © 2016 Wiley Periodicals, Inc. J. Appl. Polym. Sci. **2016**, *133*, 43950.

KEYWORDS: flame retardance; polyolefins; thermal properties; thermogravimetric analysis

Received 11 February 2016; accepted 13 May 2016
DOI: 10.1002/app.43950

INTRODUCTION

Polyethylene (PE) is widely used in many fields such as packing materials, wire, and cable covering materials due to its good flexibility at low temperatures, chemical stability, low toxicity, easy processing, and excellent electric insulation properties. However, there are some disadvantages such as low melting point and flammability, which limits its applications. Therefore, flame retardant and anti-dripping modifications are needed to meet the requirements.[1]

Halogen-based flame retardants, mineral fillers, and intumescent flame retardants (IFRs) are used in common for flame retardant modification of PE.[1–3] Halogen-based flame retardants are once the most commonly used organic flame retardants with excellent flame retardant properties, and they perform gas phase flame retardant mechanism. However, most halogen-based flame retardants are now considered gradually to be replaced owing to the environmental consideration.[1,2] Mineral fillers, such as aluminum hydroxide (ATH) and magnesium hydroxide (MH), are considered as environmental friendly flame retardant additives in PE, but their high loadings lead to great destroy of mechanical properties.[3] IFR additives are deemed to be more promising candidates with "green" character compared with halogen-based flame retardants. Common intumescent system is organic systems, and composed by an acid source, a charring agent and a foaming agent. The first used IFR system containing polyphosphate (APP)/pentaerythritol/melamine is used in PP and PE systems successfully.[4–11] Unfortunately, the traditional IFR additives also have shortcomings, especially lower water resistance, lower thermal stability, and lower flame retardant efficiency. Thus, it is essential to develop the new IFR with higher efficiency of flame retardant and smoke suppressants. Recently, triazine derivates used as charring and forming agents in IFR have been investigated, and they are excellent charring agents, which can be contributed to the presence of the triazine rings.[12–15]

In this work, a char-forming agent (CNCO-HA) containing triazine ring was synthesized and combined with APP to modify flame retardant properties of low density polyethylene (LDPE) (seen Scheme 1), which is expected to have good thermal stability, excellent water resistance and char formation ability due to the presence of the triazine rigid ring.[16] The synergistic effect of CNCO-HA and APP on the flame retardancy of LDPE systems has been investigated.

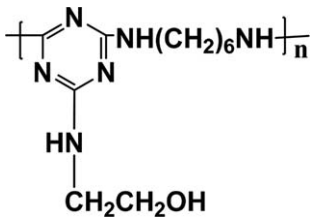

Scheme 1. Structure of CNCO-HA.

EXPERIMENTAL

Materials

LDPE resin (951-050) was produced by Maomin Petroleum Chemical Company with melt flow rate 2–2.5 g/10 min. The Ammonium polyphosphate (APP) was purchased from Shenzhen Anzheng Chemicals Company, China. The char-foaming agent (CNCO-HA) was synthesized in our laboratory[13] and its structure is shown in Scheme 1. The Antioxidant 1010 was produced by Ciba Specialty Chemicals, Switzerland.

Preparation

The flame retardant LDPE composites (LDPE/IFR) were prepared by melt blending at 110–120 °C by mixing LDPE, char-foaming agent (CNCO-HA), APP, and a small amount of antioxidant in the two-roll mill, and the mass ratio of APP to CNCO-HA was various from 4:1 to 1:1. The mixing time was 8 min for each sample with a rotor speed of 60 rpm. Then the composites were pressed on a curing machine for about 2 min to produce various thick sheets with different dimension for the tests.

Limited Oxygen Index and UL-94 Tests

The limited oxygen index (LOI) tests of all the samples were performed at room temperature by an oxygen index instrument (DRK304B) produced by Jinan Deruike Instrument Factory according to the ISO 4589 standard with the dimensions of all the samples were 130 × 10 × 4 mm^3. The vertical burning tests (UL-94) of all composites were measured by a CZF-3 instrument (Jiangning Analysis Instrument Factory), with the sample dimensions of 125 × 12.5 × 3.2 mm^3.

Thermalgravimetric Analysis

TA Q500 thermogravimetric analyzer was occupied for thermogravimetric analysis (TGA) at a heating rate of 10 °C min^{-1}. About 10 mg sample was examined under air flow rate of 40 mL min^{-1} at temperatures ranging from 35 to 800 °C. All the thermal degradation data were obtained from TG and differential thermal gravity (DTG) curves.

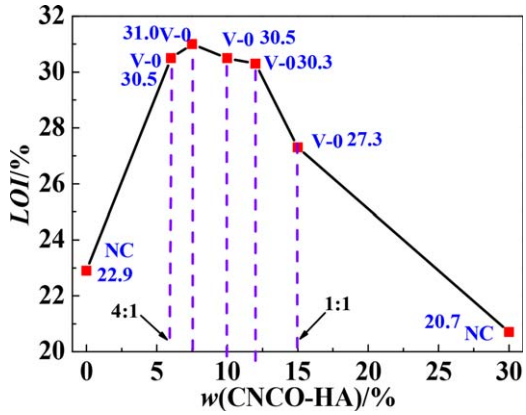

Figure 1. Effect of CNCO-HA on flame retardancy of LDPE/IFR systems. [Color figure can be viewed in the online issue, which is available at wileyonlinelibrary.com.]

Cone Calorimeter Test

Cone calorimeter test (CCT) tests were performed by the Cone Calorimeter (manufactured by Fire Testing Technology) at a heat flux of 35 kW m^{-2} in accordance with the ISO 5660-1 standard with samples dimension 100 × 100 × 4 mm^3.

Laser Raman Spectroscopy Analysis

The Laser Raman spectroscopy (LRS) measurements were carried out at room temperature with a Renishaw inVia Raman microspectrometer with excitation by a 514.5 nm helium-neon laser line focusing on a micrometer spot on the sample surface, and scanning in the 50–4000 cm^{-1} region. To avoid sample heating, the power was kept below 4 mW, and the subsequent visual examination of the surface was made to ensure no alteration happened around the focal point.

Fourier Transform Infrared Spectra Analysis

The Fourier transform infrared (FTIR) spectra were obtained with a Nicolet FTIR 6700 infrared spectrophotometer, where the samples were prepared with KBr pellets.

Scanning Electron Microscopy

The scanning electron microscopy (SEM) was performed using a SU8010 SEM to examine the morphology of the char residue obtained after treated by muffle at 500 °C for 5 min, whose

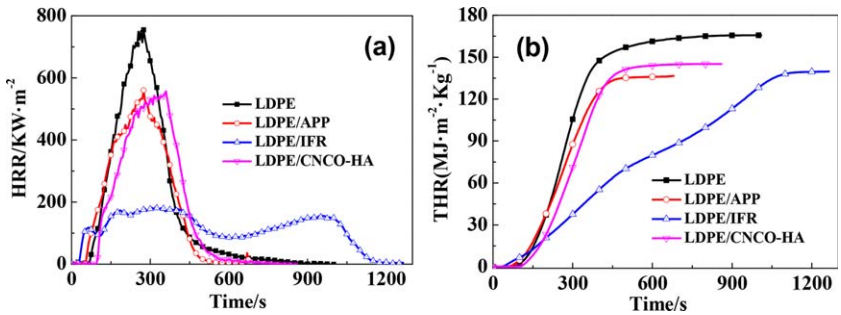

Figure 2. The HRR (a) and TSP (b) curves of LDPE and LDPE/IFR composites. [Color figure can be viewed in the online issue, which is available at wileyonlinelibrary.com.]

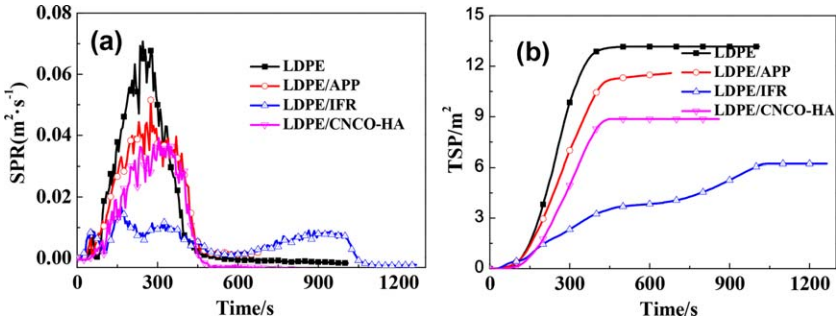

Figure 3. The SPR (a) and TSP (b) curves of LDPE and LDPE/IFR composites. [Color figure can be viewed in the online issue, which is available at wileyonlinelibrary.com.]

accelerating voltage was 15 kV. High magnification (≥5000 times) micrographs were obtained with the accelerating voltage of 2 kV and without sputter-coated platinum.

RESULTS AND DISCUSSION

Flame Retardancy of LDPE Composites

Figure 1 presented the LOI values and vertical burning rates of the LDPE/IFR composites containing 30% IFR with different APP and CNCO-HA weight ratio. The LOI value of LDPE was only 17.0%, and it was easily flammable. Only additive of 30% APP or CNCO-HA showed poor flame retardancy of LDPE with the LOI value 22.9% and 20.7% respectively, and they did not class UL-94 rating. When CNCO-HA was combined with APP together, the LOI value of LDPE composites improved dramatically with the increasing of CNCO-HA content. When the weight ratio of APP to CNCO-HA was 3:1, the LOI value of LDPE/IFR composites reached the largest value (31.0%). And then, the LOI value decreased quickly when the content of CNCO-HA increased. The experimental results of vertical testing showed that all of the LDPE/IFR composites reached V-0 rating when the weight ratio of APP and CNCO-HA was between 4:1 and 1:1. It was concluded that an appropriate weight ratio of APP to CNCO-HA in the IFR system played an important part to its flame retardancy, and an obvious synergistic effect existed between APP and CNCO-HA for LDPE.[12,16] The LDPE composites with 30% APP, CNCO-HA, or IFR were occupied for further investigation.

Combustion Behavior of LDPE and Its Composites

The CCT analysis is regarded as a powerful tool to evaluate the flame retardant properties of flame retardant materials.[18,19] It gives the following principal parameters: the heat release rate (HRR), peak heat release rate (PHRR), total heat release (THR), mass loss (ML), smoke produce rate (SPR), and total smoke produce (TSP) to predict the fire hazard.[13–16] Figures 2–5 and Table I presented the plots and data for LDPE, LDPE/APP with 30% APP, LDPE/APP with 30% CNCO-HA, and LDPE/IFR with 30% IFR obtained from the CCT.

The HRR is one of most important parameter for evaluate flame retardant properties, and it is used to express the fire intensity and fire spread rate. Figure 2(a,b) showed the HRR curves of the LDPE, LDPE/APP, LDPE/CNCO-HA, and LDPE/IFR composites. LDPE was burnt very fast after ignition with the maximum HRR value of 755 kW m^{-2} at 275 s. When 30% APP, CNCO-HA, or IFR was incorporated into LDPE, the PHRR was decreased, and the combustion time of the composites was prolonged as compared to the pure LDPE. The PHRR values of LDPE/APP and LDPE/IFR were 560, 556, and 183 kW m^{-2}, which were 25.8, 26.4, and 75.8% lower than that of LDPE, respectively. Furthermore, it can be seen that the HRR curve of LDPE/IFR became flatter than those of LDPE, LDPE/CNCO-HA, and LDP/APP during the combustion, which demonstrated that LDPE burnt more slowly and gently as IFR was introduced. It was noteworthy that the HRR curve of the LDPE/IFR presented three peaks [as shown in Figure 2(a)] while the other two composites only had one peak. It was explained as following: first, the IFR degraded and an poor intumescent shield formed; second, the intumescent coating formed at the first step was not strong enough to resist heat from the cone calorimeter and further degraded to form a new char layer with a new peak of HRR; however, the second-formed char layer was also damaged to release more heat and formed a new intumescent shield, showing the third HRR peak.[14–16]

Figure 2(b) presented the THR curves of three samples, and the THR curves of samples showed considerable differences. The neat LDPE released a total heat of 165 MJ m^{-2}, whereas the THR values of LDPE/APP, LDPE/CNCO-HA, and LDPE/IFR decreased to 136, 145, and 140 MJ m^{-2} with the reduction by 17.6, 12.1, and 15.2%, respectively. Although the THR value of

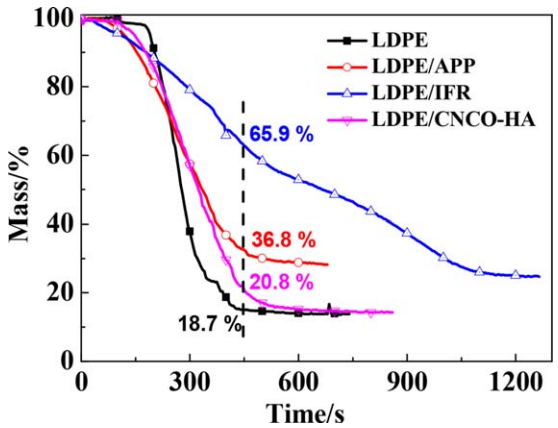

Figure 4. The Residual Mass curves of LDPE and LDPE/IFR composites. [Color figure can be viewed in the online issue, which is available at wileyonlinelibrary.com.]

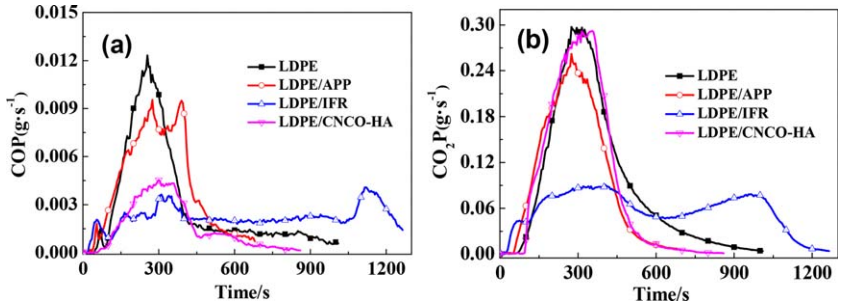

Figure 5. The COP (a) and CO2P (b) curves of LDPE and LDPE/IFR composites. [Color figure can be viewed in the online issue, which is available at wileyonlinelibrary.com.]

LDPE/IFR was a little higher than those of LDPE/APP, the curve slope of THR for LDPE/IFR was much lower than those of LDPE and LDPE/APP, which indicated that the intumescent char decreased the heat releasing rate of composites.

The SPR and total smoke release are two indicative parameters of smoke.[16,17] Figure 3(a,b) showed the SPR and TSP plots of LDPE, LDPE/APP, LDPE/CNCO-HA, and LDPE/IFR composites. The curves of SPR and TSP were similar to those of HRR

Table I. Cone Results of Flame Retardant Materials

Properties	LDPE	LDPE/APP	LDPE/CNCO-HA	LDPE/IFR
Peak1-HRR (KW m^{-2})	755	560	556	117
$t_{peak1\text{-}HRR}$ (s)	275	275	360	65
Peak2-HRR (KW m^{-2})	—	—	—	183
$t_{peak2\text{-}HRR}$ (s)	—	—	—	320
Peak3-HRR (KW m^{-2})	—		—	156
$t_{peak3\text{-}HRR}$ (s)	—		—	955
AHRR (KW m^{-2})	175		186	112
THR (MJ m^{-2} Kg)	165	136	145	140
Peak1-SPR (m^2 s^{-1})	0.009	0.05	0.04	0.009
$t_{peak1\text{-}SPR}$ (s)	60	275	305	55
Peak2-SPR (m^2 s^{-1})	0.071		—	0.017
$t_{peak2\text{-}SPR}$ (s)	245		—	165
Peak3-SPR (m^2 s^{-1})	—		—	0.012
$t_{peak3\text{-}SPR}$ (s)	—		—	325
Peak4-SPR (m^2 s^{-1})	—		—	0.009
$t_{peak4\text{-}SPR}$ (s)	—		—	865
TSP (m^2)	13.1	11.5	8.9	6.2
Peak1-COP (m^2 s^{-1})	0.0015	0.0018	—	0.0021
$t_{peak1\text{-}COP}$ (s)	70	55	—	55
Peak2-COP (m^2 s^{-1})	0.012	0.0095	0.0045	0.0025
$t_{peak2\text{-}COP}$ (s)	255	275	300	165
Peak3-COP (m^2 s^{-1})	—	0.0095	—	0.0036
$t_{peak3\text{-}COP}$ (s)	—	390	—	310
Peak4-COP (m^2 s^{-1})	—		—	0.0041
$t_{peak4\text{-}COP}$ (s)	—		—	1120
Peak1-CO_2P (m^2 s^{-1})	0.30	0.26	0.29	0.043
$t_{peak1\text{-}CO2P}$ (s)	275	275	355	65
Peak2-CO_2P (m^2 s^{-1})	—	—	—	0.089
$t_{peak2\text{-}CO2P}$ (s)	—	—	—	320
Peak3-CO_2P (m^2 s^{-1})	—	—	—	0.079
$t_{peak3\text{-}CO2P}$ (s)	—	—	—	965
Char residue at 400 s (%)	18.7	36.8	20.8	65.9

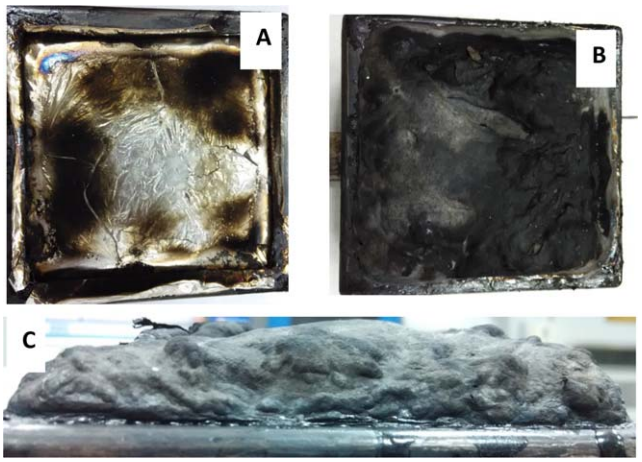

Figure 6. Photographs of the specimens after CCT of (a) LDPE, (b) and (c) LDPE/IFR. [Color figure can be viewed in the online issue, which is available at wileyonlinelibrary.com.]

and THR for the three samples, respectively. The peak SPR value of LDPE/IFR was 0.017 m^2 s^{-1}, which was 76.1, 57.5, and 66.0% lower than those of LDPE and LDPE/APP, respectively. TSP values of LDPE/IFR are 52.7, 30.3, and 46.1% lower than those of pure LDPE and LDPE/APP. These results suggested that the IFR system played a crucial role in suppressing the smoke emission owing to the stable char layer formed.

The ML curves of LDPE, LDPE/APP, LDPE/CNCO-HA, and LDPE/IFR composites were illustrated in Figure 4. Pure LDPE lost its weight quickly, and the curve slope value was large. When APP and IFR was introduced into LDPE, the composites had lower ML rate than that of LDPE with higher char residue. The char residue of LDPE/IFR was 65.9% at 450 s, which was much higher than those of the other samples (LDPE and LDPE/APP). This result suggested that IFR formed more char residue, which protected the underlying material from further degradation.

Figure 5(a,b) gave the CO production rate (COP) and CO_2 production rate (CO_2P) curves of LDPE, LDPE/APP, LDPE/CNCO-HA, and LDPE/IFR composites. The COP and CO_2P plots of four samples were similar to those of SPR and TSP plots of samples. As shown in Figure 5(a), the peak values of LDPE/APP, LDPE/CNCO-HA, and LDPE/IFR were lower than that of LDPE. At the end of burning, LDPE/IFR presented a COP peak. The LDPE/IFR composite had the lowest value as shown in the CO_2P curves of Figure 5(b). The CO_2P value of LDPE/APP, LDPE/CNCO-HA, and LDPE/IFR is 13.3, 3.3, and 85.7% lower than that of pure LDPE. These results demonstrated that IFR suppressed the production of CO_2 and CO.

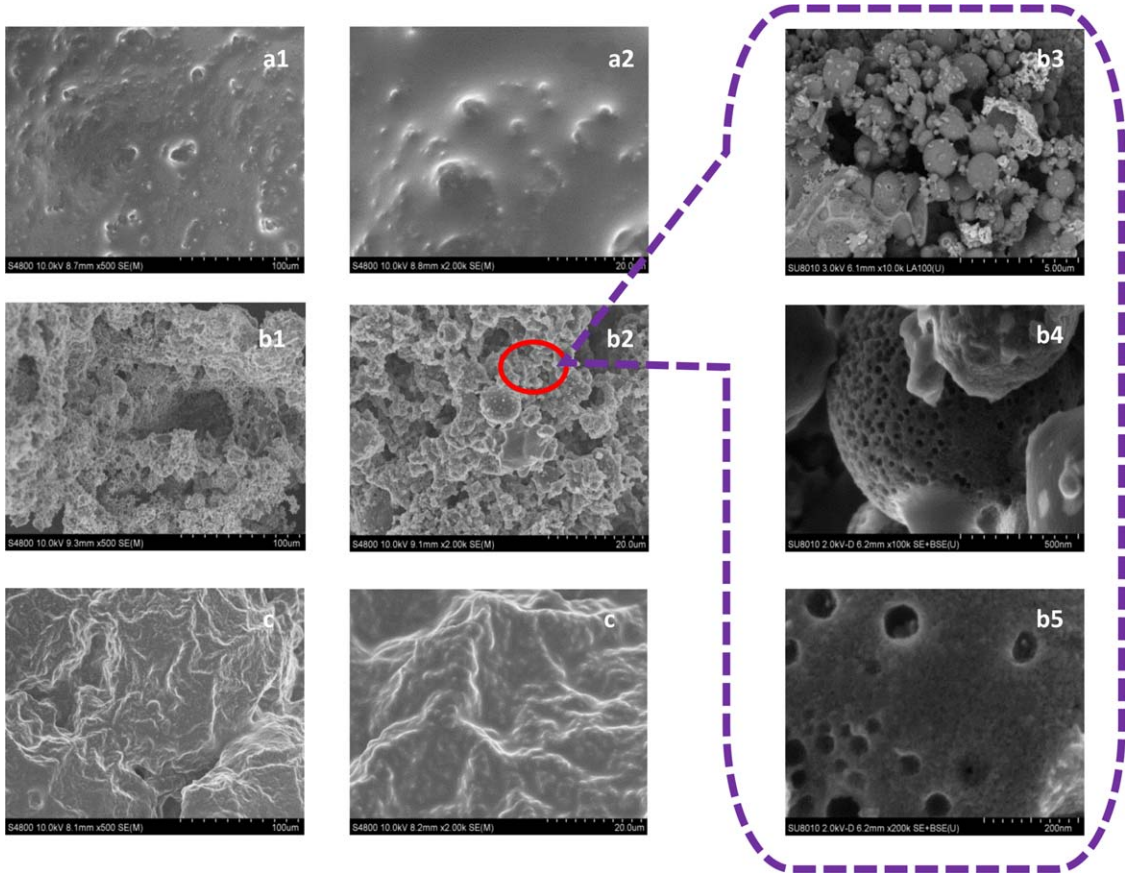

Figure 7. SEM micrographs of LDPE/APP (a1 × 500, a2 × 2000), LDPE/CNCO-HA (b1 × 500, b2 × 2000, b3 × 10k, b4 × 100k, b5 × 200k), and LDPE/IFR (c1 × 500, c2 × 2000) after heated at 500 °C for 5 min. [Color figure can be viewed in the online issue, which is available at wileyonlinelibrary.com.]

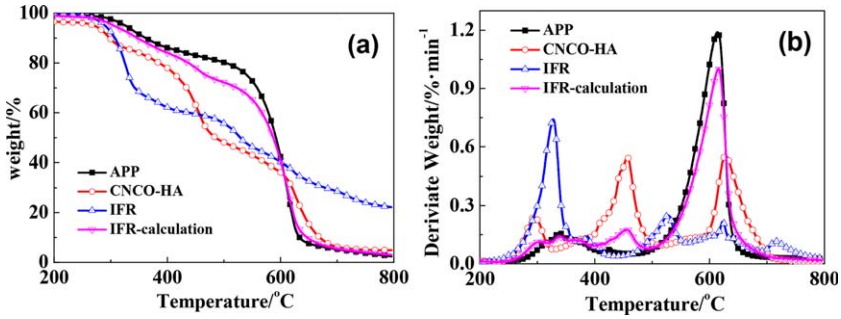

Figure 8. TGA (a) and DTG (b) curves of flame retardant agents under air. [Color figure can be viewed in the online issue, which is available at wileyonlinelibrary.com.]

Figure 6 presented the digital photos of the residues of LDPE and LDPE/IFR after the CCT. LDPE left almost nothing after burning, while a thick and intumescent char layers was formed in the case of LDPE/IFR composite, which prevented heat and mass from transferring from the flame zone to the burning substrate.

These results indicated that the IFR containing APP and CNCO-HA led to the formation of a higher quality char layer during combustion. The char layer protected the matrix effectively from heat and flammability gas penetrating and its further degradation. Consequently, the heat and smoke evolved in tests diminished obviously.[16]

Morphology of Char Residue

The microstructure of intumescent chars plays an important part to the flame retardant properties of materials, therefore, the intumescent char residue of LDPE/APP, LDPE/CNCO-HA, and LDPE/IFR with 30% additives are investigated by SEM and magnified by 500 and 2000 times, Figure 7 presented the SEM photos of composites. In case of LDPE/APP, the char layer was compact without any hole, but it did not form an intumescent char layer. So it had a dissatisfying flame retardant property. However, a loose char layer with lots of small balls and large cracks was formed for LDPE/CNCO-HA composite, and the balls connected together with lots of gaps, which was the reason for its poor flame retardant properties. The balls covering the char layer were observed by SEM with high magnification. The balls were connecting together with a large amount of gaps, and filled with numerous small and hallow holes, which revealed that CNCO-HA formed lots of char, but they were not compact enough to prevent further combustion of materials. For LDPE/IFR composite, a relatively intumescent and compact char layer was formed with fewer cracks and voids on the surface, which effectively prevents the transferring of heat and flammable volatiles, thereby leading to better flame retardant properties.[16–18] The difference of morphology of char layers for the three composites gave further evidence that there was a synergistic effect between APP and CNCO-HA expediting to form a more compact intumescent char layer.

Thermal Degradation Behavior of IFR and LDPE Composites

Figure 8 presented the TGA (a) and DTG (b) curves of APP, CNCO-HA, IFR (APP/CNCO-HA = 3:1) and IFR (APP/CNCO-HA = 3:1) calculation, and Table II listed the TGA results. APP served as an acid source and a gas source, which catalyzed dehydration and cross-linking reaction of charring agents in IFR.[16] It had good thermal stability with high initial decomposing temperature (326 °C, $T_{5\%}$) and char residue (42.3%) at 600 °C under air. CNCO-HA was used as a charring and forming agent, and it had high char residue (36.2% at 600 °C under air) and its initial decomposing temperature (313 °C, $T_{5\%}$).[16] IFR was composed by APP and CNCO-HA with weight ratio of 3:1, and it presented a little lower thermal stability with its initial decomposing temperature of 290 °C, based on 5% ML under air. IFR presented excellent thermal stability at high temperature, and its char residues at 600, 700, and 800 °C were 40.2, 28.6, and 22.2%, respectively.

In Figure 8, the IFR curve was the experimental result, and the IFR calculation curve was the result calculated from the experimental results of APP and CNCO-HA based on their percentage in the IFR system in accordance with formula (1). According to Figure 8, the thermal degradation behavior of IFR is classified into four steps, which was different to the APP, CNCO-HA, or IFR calculation curves. The main degradation peak of IFR took place at 328 °C, which was much lower than the theoretical value (615 °C), and the char residue of IFR at 700 and 800 °C was much higher than those of APP, CNCO-HA, and IFR calculation, while it was only 5.5 and 3.1% based on the calculation results. These results indicated that when APP and CNCO-HA was combined together, the thermal degradation behaviors of

Table II. TGA Data of IFR under Air

	APP	CNCO-HA	IFR[a]	IFR Calculation[b]
[c]$T_{5\%}$ (°C)	326	271	290	306
[c]$T_{10\%}$ (°C)	362	298	308	347
[c]$T_{50\%}$ (°C)	592	485	529	587
T_p (°C)	338	457	328	615
[d]$W_{600\,°C}$ (%)	42.3	36.2	40.2	40.7
[d]$W_{700\,°C}$ (%)	5.29	6.2	28.6	5.5
[d]$W_{800\,°C}$ (%)	2.44	5.0	22.2	3.1

[a] IFR is composed by APP and CNCA-DA, and the mass ratio of APP:CNCO-HA is 3:1.
[b] $W_{calculation} = W_{APP} \times 75\% + W_{CNAO\text{-}HA} \times 25\%$……(2).
[c] $T_{5\%}$, $T_{10\%}$, and $T_{50\%}$ are the temperatures at which 5%, 10%, and 50% weight loss occurs, respectively.
[d] $W_{600\,°C}$ (%), $W_{700\,°C}$ (%), and $W_{800\,°C}$ (%) are the residue of materials at 600, 700, and 800 °C.

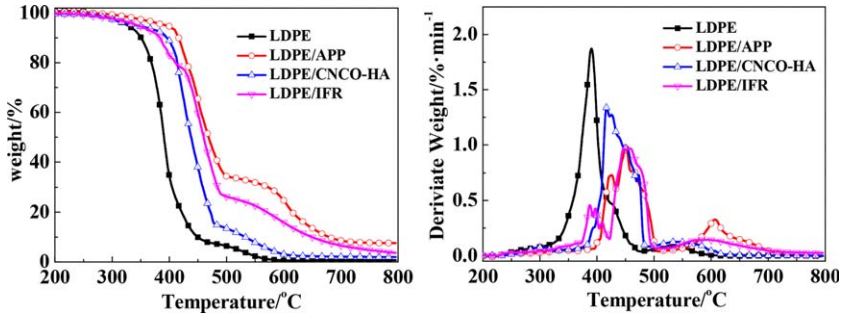

Figure 9. TGA (a) and DTG (b) curves of LDPE and LDPE composites under air. [Color figure can be viewed in the online issue, which is available at wileyonlinelibrary.com.]

APP and CNCO-HA changed to form more char layer at higher temperature.

$$w_{calculation} = w_{APP} \times 75\% + w_{CNCO-HA} \times 25\% \quad (1)$$

The TGA and DTG curves and results of LDPE, LDPE/APP LDPE/CNCO-HA, and LDPE/IFR composites with additive content of 30% under air were presented in Figure 9, and the results of them were listed in Table III. LDPE degraded rapidly with a sharp decomposition peak happened at 390 °C, whose char residue was only 0.5% at 800 °C. When APP, CNCO-HA, and IFR were introduced into LDPE, the LDPE/APP, LDPE/CNCO-HA, and LDPE/IFR composites had better thermal stability according to $T_{5\%}$, $T_{10\%}$, and $T_{50\%}$. The curves of three composites obviously shifted to higher temperature due to the degradation of a char layer formed by APP, CNCO-HA, and IFR. Especially, when APP and CNCO-HA were combined together, the LDPE/IFR composite had much higher thermal stability with higher thermal degradation temperature according to $T_{5\%}$, $T_{10\%}$, and $T_{50\%}$, which were assigned to the char layer formed by IFR. Meanwhile, all the flame retardant composites had higher char residue than that of LDPE, and the LDPE/IFR had the highest value, whose the char residue reached 15.9, 6.6, and 3.6% at 600, 700, and 800 °C, respectively. These facts indicated that there was a synergism between APP and CNCO-HA, and IFR formed more char to restrain the thermal degradation of composites.

Table III. TGA Data of LDPE/IFR Systems under Air

	LDPE	LDPE/APP	LDPE/CNCO-HA	LDPE/IFR[a]
[b]$T_{5\%}$ (°C)	328	344	343	344
[b]$T_{10\%}$ (°C)	351	367	396	384
[b]$T_{50\%}$ (°C)	391	466	438	460
[c]T_p (°C)	390	439	417	448
[d]$W_{600\,°C}$ (%)	0.6	19.7	3.1	15.9
[d]$W_{700\,°C}$ (%)	0.6	7.5	2.1	6.6
[d]$W_{800\,°C}$ (%)	0.5	6.0	2.0	3.6

[a] The mass ratio of APP:CNCO-HA is 3:1, and mass fraction of IFR is 30%.
[b] $T_{5\%}$ and $T_{10\%}$ and $T_{50\%}$ are the temperature at which 5% and 10% and 50% weight loss occurs, respectively.
[c] T_p is the temperature at which the maximum of weight loss rate take place.
[d] $W_{600\,°C}$ (%), $W_{700\,°C}$ (%), and $W_{800\,°C}$ (%) are the residue of materials at 600, 700, and 800 °C.

FTIR and LRS Analysis for Final Chars

The LRS has been usually occupied to evaluate the graphitization degree of the residue char, which plays a significant role in the strength and thermal stability of the char layer. The peak occurred at about 1380 cm^{-1} (D-band) showed the unorganized carbon structure, and the peak happened at about 1600 cm^{-1} (G-band) represents the graphitic structure.16,18 Figure 10 presented the Raman spectra of chars for LDPE/APP, LDPE/CNCO-HA, and LDPE/IFR composites and there were two characteristic peaks in the every spectrum, which demonstrated that there were unorganized carbon structure and graphitic structure in the char layers.

Each spectrum of char was subject to peak fitting using the curve fitting software Origin 8.5/Peak Fitting Module to divide the curve into 2 Gaussian peaks. The ratio (R) of the integral peak intensity of the D band and G band, $R = A_D/A_G$, represents the graphitization degree of the char. The lower the value of R was, the higher graphitization degree of char formed, which presented better shield protection of the char layer from combustion.[15,16] The integrated calculation results of the three samples after treated at 500 °C for 5 min were listed Table IV. The R values of LDPE/APP, LDPE/CNCO-HA, and LDPE/IFR were 2.94, 2.70, and 1.91. These results further indicated that when

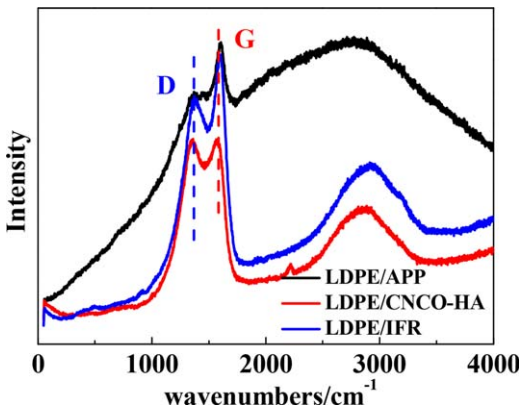

Figure 10. Raman spectra of char residues of LDPE/APP, LDPE/CNCO-HA, and LDPE/IFR composites. [Color figure can be viewed in the online issue, which is available at wileyonlinelibrary.com.]

Table IV. Results of Raman Analysis of Char Residues for LDPE/APP, LDPE/CNCO-HA, and LDPE/IFR

Sample	A_D	A_G	$R = A_D/A_G$
LDPE/APP	796,359	271,066	2.94
LDPE/CNCO-HA	2,188,666	811,979	2.70
LDPE/IFR	2,504,056	1,312,268	1.91

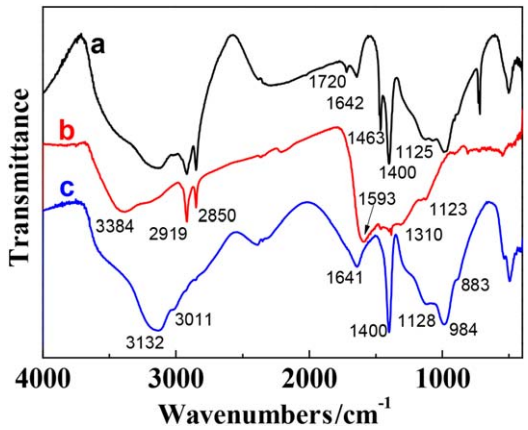

Figure 11. FTIR spectra of char residues of (a) LDPE/APP, (b) LDPE/CNCO-HA, and (c) LDPE/IFR composites. [Color figure can be viewed in the online issue, which is available at wileyonlinelibrary.com.]

APP and CNCO-HA combined together, proper proportion of graphitization promoted to form more perfect char layer with higher graphitization degree.

FTIR was used to characterize the chemical compositions of the final chars of composites after treated at 500 °C for 5 min, as shown in Figure 11. The band at among 3384–3132 cm^{-1} was assigned to stretching vibration of —NH and —OH.[19] Bands at 2919 and 2850 cm^{-1} were contributed to —CH_2— structure. The bands appearing at around 1641 cm^{-1} were assigned to C=C absorption of polyaromatic structure.[19] Bands at about 1400 cm^{-1} in the curve of LDPE/APP and LDPE/IFR were attributed to P—N structure, the peak at 1276 cm^{-1} belonged to P=O structure, and peaks at about 1125 cm^{-1} was attributed to P—O bond in P—O—P structure, and bands around 984 and 884 cm^{-1} were assigned to P—O bond in P—O—C structure.[20] Compared to the LDPE/APP and LDPE/CNCO-HA, the difference of the bands was at about 1400 and 1641 cm^{-1} which were assigned to P-N and C=C structure.[21,22] The FTIR spectrum from LDPE/IFR confirmed the existence of P—O—P, P—O—C, and P—N structure in char, which suggested that the cross-linking structures of P—O—P and P—O—C were formed by the reaction between APP and CNCO-HA during combustion.

CONCLUSIONS

An oligomeric charring agent CNCO-HA containing a triazine ring was chosen, and the combination of APP and CNCO-HA formed an effective IFR system for LDPE. When the mass ratio of APP and CNCO-HA was 3:1, the LDPE/IFR composite reached the highest value 31.0% with 30% IFR loading. At this optimum ratio, LDPE/IFR composite presented a LOI value of 26.8% and UL-94 V-0 rating with 25% IFR loading. In case of cone calorimeter studies, IFR reduced the flammability and smoke production of LDPE significantly with lower value of HRR, THR, SPR, TSP, COP, CO_2P, and ML. The TGA results indicated that there was synergistic effect between APP and CNCO-HA presenting higher the char formation ability of the APP/CNCO-HA. The char residue of APP/CNCO-HA reached 40.2, 28.6, and 22.2 wt % at 600, 700, and 800 °C under air while it was only 40.7, 5.5, and 3.1 wt % in calculation. Therefore, the synergism between APP and CNCO-HA enhanced the thermal stability of LDPE. The morphological structure of the char residue observed by SEM proved that the weight ratio of APP to CNCO-HA played a critical part in the formation of a compact and homogeneous char layer on the surface during combustion, and char structure was most important factor for the flame retardant properties. The investigation of the LRS and FTIR spectroscopy revealed that APP and CNCO-HA promoted char to form a suitable content of the graphitic structure and crosslinking networks to enhance the flame retardant performance.

ACKNOWLEDGMENTS

The financial supports by National Natural Science Foundation of Guangdong China (2014A030310316) and Foundation for Distinguished Young Teachers in Higher Education of Guangdong China (YQ2014001) are gratefully acknowledged.

REFERENCES

1. Xie, F.; Wang, Z.; Yang, B.; Liu, Y. *Macromol. Mater. Eng.* **2006**, *291*, 247.
2. Le Bras, M.; Bugajny, M.; Lefebvre, J. M.; Bourbigot, S. *Polym. Int.* **2000**, *49*, 1115.
3. Hippi, U.; Mattila, J.; Korhonen, M.; Seppälä, J. *Polymer* **2003**, *44*, 1193.
4. Bellayer, S.; Tavard, E.; Duquesne, S.; Piechaczyk, A.; Bourbigot, S. *Polym. Degrad. Stabil.* **2009**, *94*, 797.
5. Bourbigot, S.; Le Bras, M. *Carbon* **1995**, *33*, 283.
6. Chiu, S. H.; Wang, W. K. *Polymer* **1998**, *39*, 1951.
7. Camino, G.; Costa, L.; Trossarelli, L. *Polym. Degrad. Stabil.* **1985**, *12*, 213.
8. Riva, A.; Camino, G.; Fomperie, L.; Amigouet, P. *Polym. Degrad. Stabil.* **2003**, *82*, 341.
9. Camino, G.; Costa, L.; Trossarelli, L. *Polym. Degrad. Stabil.* **1984**, *6*, 243.
10. Camino, G.; Costa, L.; Trossarelli, L. *Polym. Degrad. Stabil.* **1985**, *12*, 203.
11. Camino, G.; Martinasso, G.; Costa, L. *Polym. Degrad. Stabil.* **1990**, *27*, 285.
12. Hu, X. P.; Li, W. Y.; Wang, Y. Z. *J. Appl. Polym. Sci.* **2004**, *94*, 1556.
13. Feng, C. M.; Zhang, Y.; Liu, S. W.; Chi, Z. G.; Xu, J. R. *J. Appl. Polym. Sci.* **2012**, *123*, 3208.

14. Dai, J. F.; Li, B. *J. Appl. Polym. Sci.* **2010**, *116*, 2157.

15. Feng, C. M.; Liang, M. Y.; Jiang, J.; Huang, J. G.; Liu, H. B. *J. Anal. Appl. Pyrolysis.* **2016**, *118*, 9.

16. Feng, C. M.; Li, Z. W.; Liang, M. Y.; Huang, J. G.; Liu, H. B. *J. Anal. Appl. Pyrolysis* **2015**, *111*, 238.

17. Hu, X. P.; Li, Y. L.; Wang, Y. Z. *Macromol. Mater. Eng.* **2004**, *289*, 208.

18. Tuinstra, F.; Koenig, J. L. *J. Chem. Phys.* **1970**, *53*, 1126.

19. Zhou, S.; Song, L.; Wang, Z. Z.; Hu, Y.; Xing, W. Y. *Polym. Degrad. Stabil.* **2008**, *93*, 1799.

20. Su, X. Q.; Yi, Y. W.; Tao, J.; Qi, H. Q.; Li, D. Y. *Polym. Degrad. Stabil.* **2014**, *105*, 12.

21. Mahapatra, S. S.; Karak, N. *Polym. Degrad. Stabil.* **2007**, *92*, 947.

22. Gorce, J.; Spells, S. J. *Polymer* **2002**, *43*, 4043.